Theor Chem Acc (2010) 125:375–386
DOI 10.1007/s00214-009-0611-3

REGULAR ARTICLE

Rationalizing perhydrolase activity of aryl-esterase and subtilisin Carlsberg mutants by molecular dynamics simulations of the second tetrahedral intermediate state

Wook Lee · Ljubica Vojcic · Dragana Despotovic · Radivoje Prodanovic · Karl-Heinz Maurer · Ulrich Schwaneberg · Martin Zacharias

Received: 24 March 2009 / Accepted: 11 July 2009 / Published online: 30 July 2009

Abstract The perhydrolysis reaction in hydrolases is an important example of catalytic promiscuity and has many potential industrial applications. The mechanisms of perhydrolase activity of a subtilisin Carlsberg mutant and of an aryl-esterase mutant have been investigated using classical molecular dynamics simulations of the second tetrahedral intermediate (TI) state. The simulations demonstrated that hydrogen bonding between the second TI of the perhydrolysis reaction is possible in the mutants but not wild type. The stabilization by hydrogen bonds was specific for the perhydrolysis intermediate and either no hydrogen bonding or only weakened hydrogen bonding to the second TI state of the hydrolysis reaction was observed. Furthermore, a significant hindrance to the formation of the catalytically important hydrogen bond between His64 and Ser221 in the catalytic triad by competing hydrogen bonds was found for the subtilisin mutant but not wild type enzyme in case of the hydrolysis intermediate. The opposite was observed in case of the perhydrolysis intermediate. The result offers a qualitative explanation for the overall reduced hydrolysis activity of the subtilisin mutant. In addition, the simulations also explain qualitatively the perhydrolysis activity of the enzyme variants and may be helpful for designing enzyme mutants with further improved perhydrolysis activity.

Keywords Molecular simulation · Enzyme promiscuity · Perhydrolysis catalysis · Intermediate stabilization

Dedicated to Professor Sandor Suhai on the occasion of his 65th birthday and published as part of the Suhai Festschrift Issue.

Electronic supplementary material The online version of this article (doi:10.1007/s00214-009-0611-3) contains supplementary material, which is available to authorized users.

W. Lee
Institute of Organic Chemistry,
University of Würzburg, 97074 Am Hubland, Würzburg

L. Vojcic · D. Despotovic · R. Prodanovic · M. Zacharias
School of Engineering and Science, Jacobs University,
Campus Ring 1, 28759 Bremen, Germany

K.-H. Maurer
WRC-Biotechnology, Henkel AG & Co. KGaA,
40191 Düsseldorf, Germany

U. Schwaneberg
RWTH Aachen, Worringerweg 1 52074 Aachen, Germany

Present Address:
M. Zacharias (✉)
Physics Department, Technical University Munich,
James Franck Str. 1, 85747 Garching, Germany
e-mail: Martin.Zacharias@ph.tum.de

1 Introduction

It is widely believed that most enzymes have evolved to be specific for a limited set of substrates and a reaction that is catalyzed. However, over the last few years, many enzymes have been found to have the ability to catalyze alternative reactions distinct from the original reactions. This ability of active site in enzymes to catalyze several different chemical reactions is called catalytic promiscuity, and it is considered as one of the most interesting phenomena in biocatalysis [1–3]. It is worth investigating the molecular reasons for catalytic promiscuity in enzymes because rational understanding of catalytic promiscuity can provide us with concepts for designing new catalyzed reaction with well-known enzymes.

One example of catalytic promiscuity is the perhydrolysis reaction catalyzed by hydrolases which is of

significant importance for several biotechnological and industrial applications [3–5]. Perhydrolysis is a reaction which uses hydrogen peroxide as a nucleophile to form peracid. Originally, the primary functions of hydrolases are cleavage of ester bonds or short chain esters as in lipases or esterases, and to hydrolyze peptide bonds as in proteases. However, it was observed that some hydrolases could also catalyze a perhydrolysis reaction [3–5]. The first finding related to this non-conventional reaction catalyzed by some hydrolases was reported in 1985 [6]. In this study, the authors observed that hydrolases working in organic media could accept nucleophiles other than water, and this result encouraged many researchers to study the use of hydrogen peroxide as a nucleophile in reactions catalyzed by hydrolases. After more than a decade, a possible molecular basis (mechanism) of perhydrolase activity in serine hydrolases was proposed [7].

In addition to hydrolases the class of haloperoxidase enzymes is also able to use hydrogen peroxide as a substrate. Haloperoxidases first catalyze the oxidation of a halide ion in the presence of hydrogen peroxide to produce the corresponding hypohalous acid. Subsequently, the hypohalous acid acts as an electrophile and reacts with suitable organic substrates to finally produce halogenated organic compounds [8, 9]. The mechanism of this process has been studied in one class of these enzymes, so called non-heme, metal-free, or cofactor-free haloperoxidases. It was indirectly proven that the perhydrolysis reaction took place as an intermediate step during the reaction process [10]. Therefore, these metal-free haloperoxidases are also termed perhydrolases.

An interesting fact concerning these metal-free haloperoxidases is that they have a Ser-His-Asp catalytic triad which is commonly found in serine hydrolases [11, 12]. Furthermore, it was also observed that several hydrolases catalyzed the perhydrolysis reaction albeit slowly when relevant substrates were used, and even showed some haloperoxidase activity [13–15]. In addition to these findings, it was also observed that some metal-free haloperoxidases could catalyze the hydrolysis reactions to a limited extent [10]. Therefore, the metal-free haloperoxidases and hydrolases were assumed to stem from a common origin and share a similar catalytic mechanism [12]. However, in spite of all these findings, it was still difficult to explain why hydrolases exhibited much lower perhydrolase activity than the hydrolase activity, while perhydrolases (metal-free haloperoxidases) displayed much lower hydrolase activity than perhydrolase activity. Additionally, the existence of serine hydrolases such as high alkaline subtilisins (e.g. Savinase^{TM}), which in contrast to alkaline subtilisins like subtilisin Carlsberg exhibit no perhydrolase activity at all, implies that the catalytic triad Ser-His-Asp alone does not solely determine the perhydrolase activity [7]. Yet the high alkaline subtilisins are also weak in ester hydrolase activity.

An interesting explanation concerning the molecular origin of the perhydrolase activity in serine hydrolases was suggested by Bernhardt et al. [7]. The authors identified residues around the catalytic center which are only conserved in the perhydrolases group and not in the esterases group by aligning the sequences from six hydrolases (without experimentally measured catalysis of the perhydrolysis reaction) and six hydrolases (with proven perhydrolase activity). Subsequently, residues were randomly mutated in the relevant positions of the aryl-esterase from *Pseudomonas fluorescens* (PFE) with only low perhydrolase activity and which showed no remarkable structural difference with respect to its homologous hydrolases that showed some perhydrolysis activity. Using this approach it was possible to obtain a 28-fold increase of perhydrolase activity in a mutant where Leu29 was substituted with Pro. Based on molecular modeling Bernhardt et al. [7] proposed that the Pro29 residue may cause a shift of the backbone oxygen of the neighboring Trp28, which in turn could form a hydrogen bond with the hydrogen atom of the perhydroxyl-group of the second tetrahedral intermediate (TI) state, stabilizing the state and promoting the perhydrolysis reaction. The mechanism of the perhydrolysis reaction in an enzyme with a Ser-His-Asp catalytic site is indicated in Fig. 1, and in Fig. 2a and b an illustration of the proposed stabilization of the second TI state is indicated.

In addition to these results, Bernhardt et al. [7] also suggested two reasons why high alkaline subtilisins do not exhibit perhydrolase activity: The first reason is the absence of an amino acid side chain or any backbone groups in the active site which could stabilize the perhydroxyl group in the second TI state. The second reason is that in the second TI state, the peroxy group may interact with the hydrogen atom of the catalytic histidine, thereby interfering with the catalytically important interaction between the oxygen atom in the catalytic serine and the hydrogen atom in catalytic histidine which is consequently inhibitory for the perhydrolysis reaction. However, subtilisin Carlsberg wild type does show some perhydrolysis activity. The efficient catalysis of the perhydrolysis reaction is of significant importance for biotechnological and industrial applications. The observation that some natural hydrolases show a weak perhydrolysis activity which can be improved by mutagenesis may offer the opportunity to generate efficient and specific perhydrolases by redesigning natural hydrolases. In case of the catalytic cycle of subtilisin Carlsberg the hydrogen peroxide substrate comes into play after the Acl-enzyme complex has been formed (Fig. 1) and therefore the specific stabilization of the second TI for the perhydrolysis reaction is of key importance for the stabilization and completion of the perhydrolysis reaction.

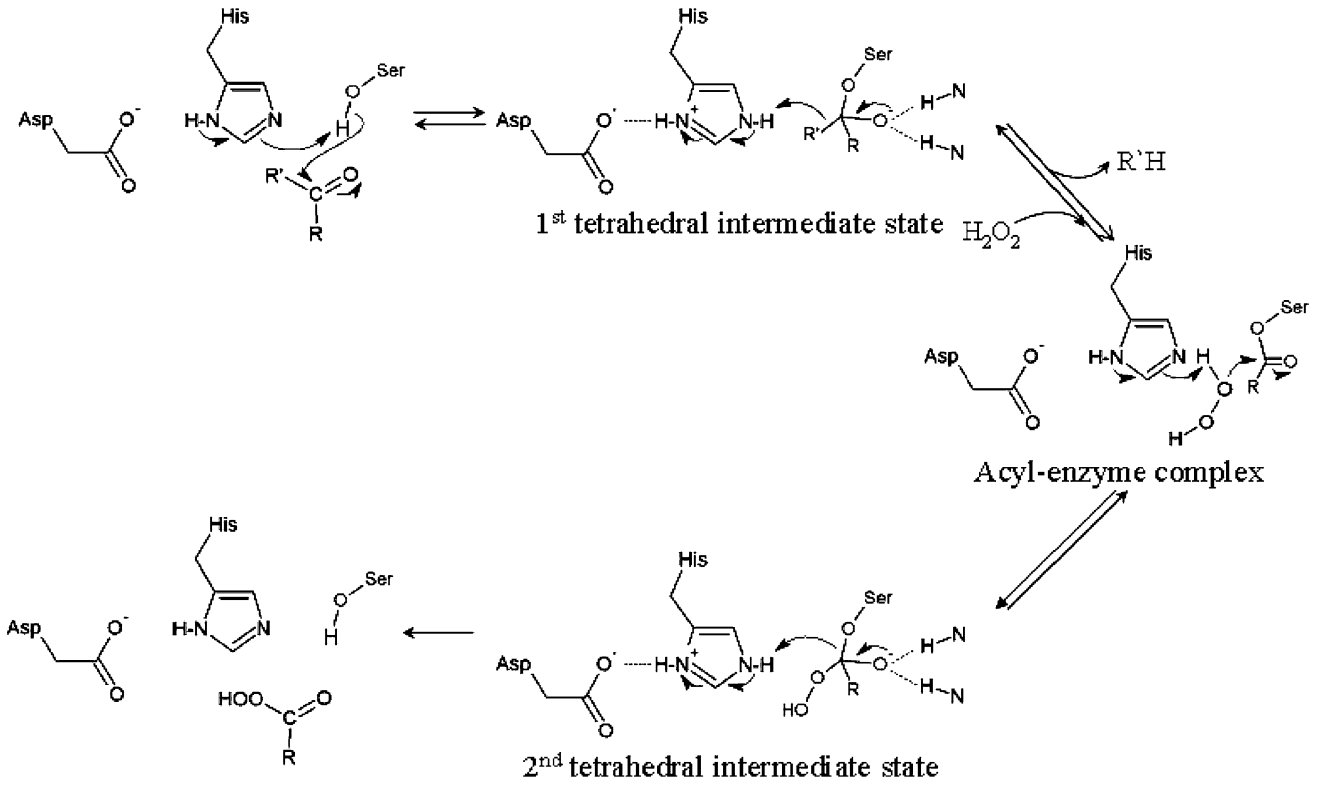

Fig. 1 Catalytic cycle for the perhydrolysis reaction in an enzyme with a Ser-His-Asp triad according to Bernhardt et al. [7]. In the case of a hydrolysis reaction a water molecule attacks the acyl-enzyme complex as a nucleophile. For the perhydrolysis reaction a hydrogen peroxide molecule attacks the acyl-enzyme complex as a nucleophile instead of a water molecule in case of the hydrolysis reaction. The reaction proceeds then like the hydrolysis reaction but a hydrogen transfer from the His Nε-H to the oxygen of Ser (OG atom) leads to the release of a peracid group (instead of a carboxy group in case of hydrolysis)

Recently, a double mutant of subtilisin Carlsberg, Thr59Ala/Leu217Trp (T59A/L217W) has been found with increased perhydrolase activity [16]. Motivated by the work of Bernhardt et al. [7], we have used molecular dynamics (MD) simulations to study the Leu29Pro (L29P) mutation in the PFE aryl-esterase and subtilisin Carlsberg (wild type and mutants) with the second TI states of the hydrolysis and of the perhydrolysis reaction. The second TI states were studied by a molecular mechanics force field. The analysis of the hydrogen bonding pattern during the simulations indicated that the Leu217Trp (L217W) substitution indeed can result in a weak hydrogen (H-)bond formation between the Tryptophan (Nε-H) and the second oxygen of the perhydroxyl group in the second TI. In contrast, the equivalent H-bond with the oxygen of the carboxyl group (in the second TI of the hydrolysis reaction) could not be formed because of the larger distance of the oxygen atom to the Trp217:Nε-H. In addition, simulations were also performed on the aryl-esterase (wildtype and L29P mutation) and gave results fully compatible with the proposed mechanism by Bernhardt et al. [7]. The simulation studies offer an explanation for the dramatic qualitative difference of the subtilisin wild type and the T59A/L217W mutant with respect to catalysis of hydrolysis and perhydrolysis reactions. The simulations may also be the basis for a further systematic and rational redesign of the subtilisin to increase its capacity for catalyzing the perhydrolysis reaction which has an enormous potential for industrial and biotechnological applications.

2 Materials and methods

2.1 Starting structures and force field setup for second tetrahedral intermediate state

The initial structures were based on the X-ray crystal structure of subtilisin Carlsberg and aryl-esterase from *P. fluorescens* (Protein Data Bank (PDB) entry 1SCD [17] and 1VA4 [15], respectively). The placement and chirality of the second TI was based on the experimentally known structure of subtilisin (Carlsberg) in complex with L-parachlorophenyl-1-acetamido boronic acid inhibitor (PDB entry 1VSB [18]) which represents a structural model for the second TI. For substitution of residues in silico the Swiss-Pdb Viewer program was used [19]. For each

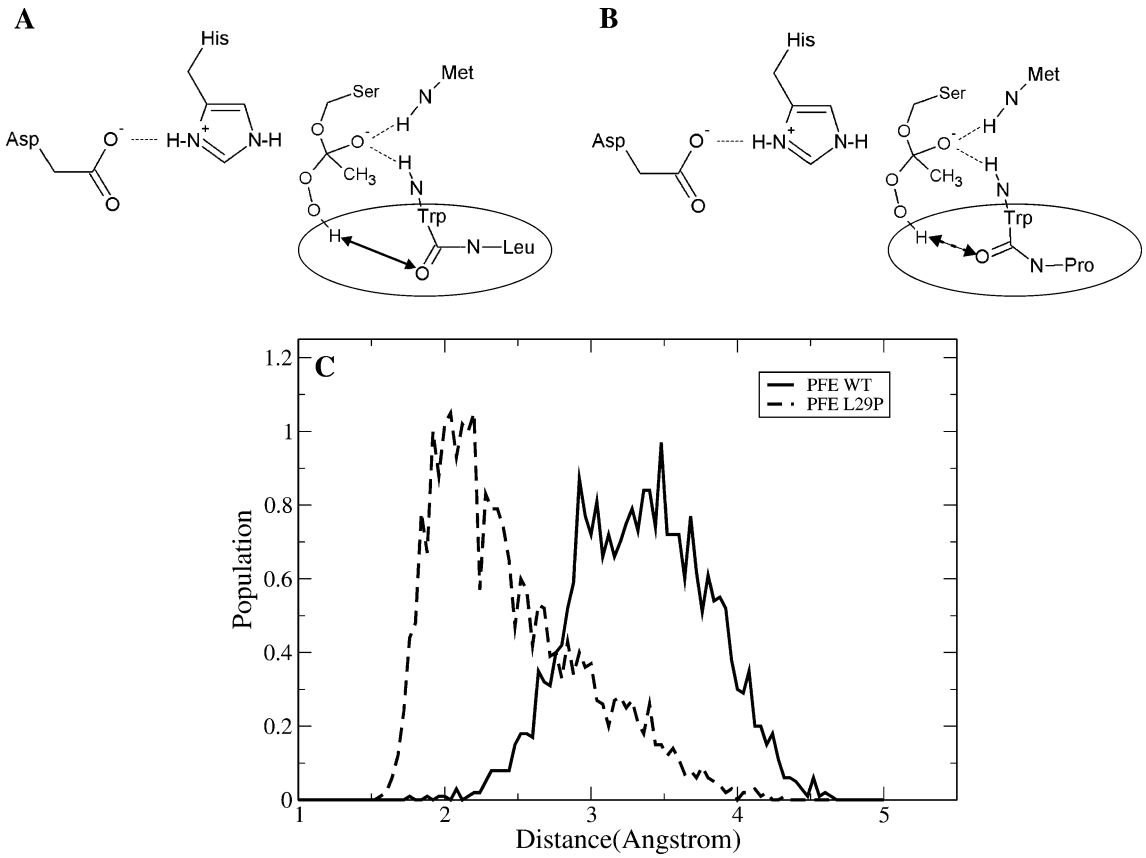

Fig. 2 Proposed molecular mechanism of perhydrolase activity in the L29P mutation of the aryl-esterase from *Pseudomonas fluorescens* (PFE) [7]. The second TI state of the PFE wild type and the L29P mutant enzymes are schematically illustrated in **a** and **b**, respectively. The replacement of the Leu29 residue by Pro was proposed to result in a slightly modified backbone structure which brings the carbonyl oxygen of Trp28 closer to the perhydroxy group and in turn allowing hydrogen bond formation [7, encircled in the Figure]. The hydrogen bonds that stabilize the intermediate state are shown as double-arrows. **c** Distance distribution curves for the interaction between the hydrogen of the peroxy group and backbone oxygen of Trp28 obtained from MD simulations of the second TI state of the perhydrolysis reaction. The curves indicate the recorded distance distribution between carbonyl oxygen of Trp28 and the hydrogen of the perhydroxy group in wild type (*continuous line*) and in the L29P mutant (*dashed line*)

mutation, the energetically most favorable rotamer was chosen.

The TI part of the second TI state of the hydrolysis and perhydrolysis reactions were generated using the Antechamber module of the AMBER 8.0 package [20] and represent a modified Ser residue. For generating partial charges for the second TI structure, quantum mechanical calculations were performed following the recommendations to derive charges for the Amber force fields [20, 21]. Quantum mechanical Hartree Fock calculations were performed with Gaussian03 [22] using the 6-31G basis set and partial charges were derived using the RESP program [23] of AMBER 8.0. As a control partial charges were also derived using the MP2/6-311++G(d,p) basis set resulting in a similar charge distribution with deviations of <5% for most RESP derived partial charges (see Table 1s in Supplementary Material). The general AMBER force field (GAFF) [24] was used to setup the bonded and non-bonded force field parameters for the second TI structure (force field parameters are listed in Tables 2s–7s in Supplementary Material).

2.2 Molecular dynamics simulations

All MD simulations were carried out using the Sander module of the Amber8 package [20] in combination with the parm03 force field [21] and including explicit solvent molecules. Each initial structure was first neutralized by adding chloride or sodium ions, then ten more chloride ions and sodium ions were added to achieve a salt concentration of approximately 100 mM. Each system was solvated in a truncated octahedron box of TIP3P water molecules [25] with a minimal distance of 10.0 Å between solute and the box boundaries. Approximately, 5,000 water molecules were added for subtilisin Carlsberg, and close to 6,000 water molecules were added in case of the aryl-esterase system. Energy minimization was performed to remove any sterical overlap for 500 steps. For the MD simulations

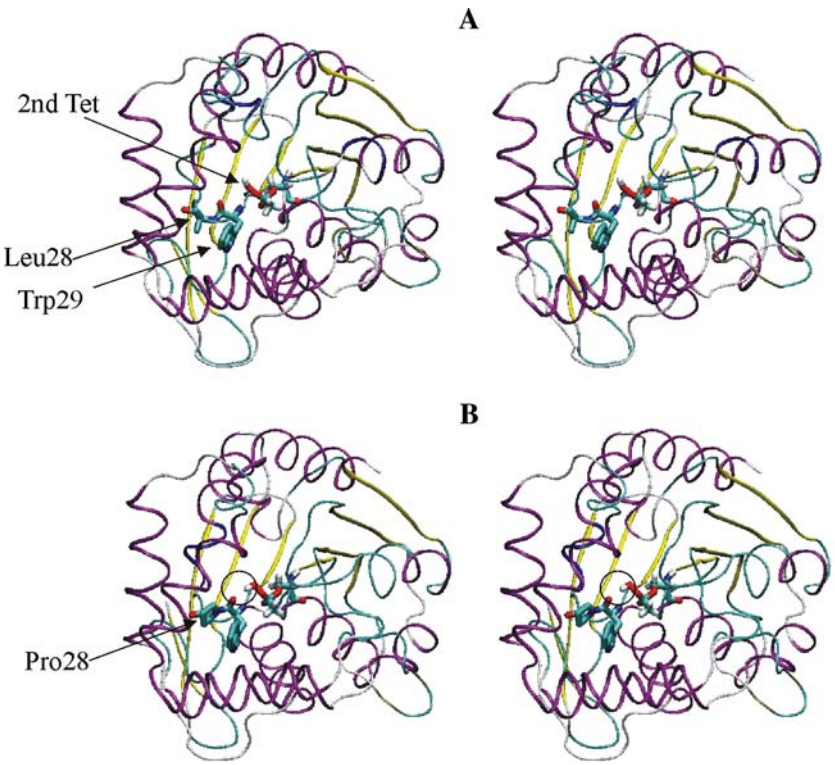

Fig. 3 Conformational snapshots (stereo views after ~1.5 ns MD simulation) of the aryl-esterase from *Pseudomonas fluorescens* wild type (**a**) and L29P mutation (**b**). The backbone is shown as secondary structure coded cartoon. Residues 28, 29 and of the second TI are in stick representation and indicated by *arrows*. The formation of a hydrogen bond between the peroxy-hydrogen of the second TI and carbonyl oxygen (of Trp28) in the mutant is encircled (in **b**)

the temperature of the systems was gradually increased from 50 to 300 K in 50 K steps as protein atoms were restrained to the initial positions with a force constant of 25 kcal mol^{-1} $Å^{-2}$. After reaching a temperature of 300 K, the restraints were gradually decreased in a stepwise manner to approach zero at the final equilibration step. The Shake algorithm [26] was used for all bonds containing hydrogen atoms allowing a time step of 2 fs. If not otherwise mentioned, the total length of all MD simulations in the present study was 5 ns. Only the last 4 ns were used for data gathering (1 ns equilibration).

3 Results and discussion

3.1 Molecular dynamics simulations of wild type aryl esterase and a L29P mutant

The stabilization of the second TI state plays a key role for the hydrolysis reaction and possible perhydrolysis reaction of hydrolytic enzymes with a Ser-His-Asp catalytic triad [7, 27–36]. In order to qualitatively test a possible mechanism for the stabilization of the second TI in case of an aryl-esterase from *P. fluorescens* by the L29P mutation suggested by Bernhardt et al. [7] comparative MD simulations on the wild type enzyme and the mutant were performed. The mutation L29P was introduced in silico using the SPDBviewer software [17, see Methods]. The Pro residue has a restricted conformation resulting in a small local rearrangement of the backbone but no alteration of the side chains. Snapshots form the MD simulations illustrate the arrangement of residues 28, 29 and the second TI in the wild type and mutant enzymes (Fig. 3). The MD simulations resulted in stable trajectories with the root mean square deviation (Rmsd of backbone) of the proteins approaching a stable level of ~1–1.5 Å after ~1 ns (not shown but similar to results shown for the simulations on subtilisin Carlsberg, Fig. 4, and see next paragraph). The final 4 ns simulation time were used as data gathering period. The distance between the hydrogen atom of the perhydroxyl group and carbonyl oxygen of residue 28 was recorded for both the wild type and L29P mutant and plotted in Fig. 2c. Clearly, in case of the mutant most of the sampled states corresponded to distances that allow a stable hydrogen bonding between the peroxy-hydrogen and the backbone carbonyl group in case of the mutant. However, for the wild type the sampled distances are considerably larger (mostly >3 Å) allowing at most for weak hydrogen bonding. The result is fully consistent with the mechanism of hydrogen bonding stabilizing of the second tetrahedral perhydrolysis intermediate state suggested by Bernhardt et al. [7] for the L29P mutant. The Pro residue at position 29 slightly rearranges the main chain structure which leads to a shift of the carbonyl oxygen of residue 28 which in turn allows the selective stabilization of the perhydrolysis intermediate and explains qualitatively the effect of the

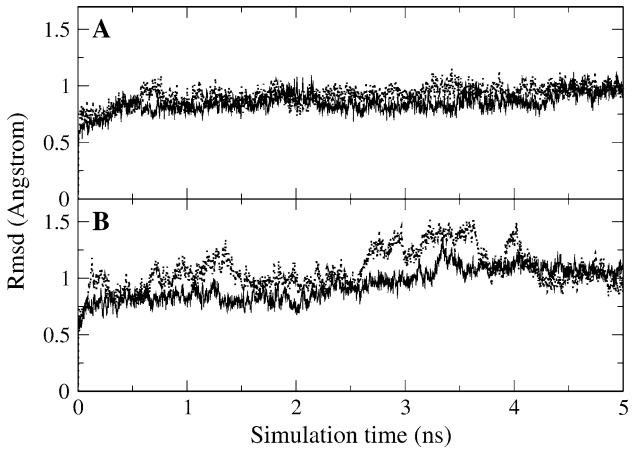

Fig. 4 Root mean square deviation (backbone Rmsd) of sampled protein conformation during equilibration (first ns) and data gathering period (last 4 ns). **a** MD simulation of subtilisin Carlsberg wildtype (*continuous line*) and T59A/L217W mutant (*dotted line*) in complex with the second intermediate for the hydrolysis reaction. **b** same as (**a**) for the simulation of the second intermediate state of the perhydrolysis reaction

mutation (see stereo views in Fig. 3). The result also indicates that the present methodology could potentially also be useful to offer an explanation for the experimentally observed perhydrolysis catalysis in case of the subtilisin Carlsberg T59A/L217W mutant.

3.2 MD simulations of subtilisin Carlsberg wild type and T59A/L217W double mutant

The initial structures for MD simulations corresponded to the X-ray crystal structure of subtilisin Carlsberg, and the T59A/L217W mutations were introduced in silico (see Methods). Visual inspection indicated that the T59A mutation is located far away from the enzyme active site. The distance between residue 59 and the second TI structure is ~18.5 Å (measured as the distance between Cα atoms of residue 59 and the catalytic Ser221 with the attached the second TI structure). The L217W substitution is located more closely to the active site triad. The Trp217 side chain conformation was systematically varied and the state with least sterical overlap was used as start structure for the subsequent simulations. Similar to the MD simulations on the aryl-esterase (previous paragraph) 5 ns explicit solvent simulations (data gathering limited to the final 4 ns of each simulation) of the wild type and mutant enzymes were performed (to control the convergence simulations were extended to 8 ns data gathering). In general, the structures stayed close to the start structure with an Rmsd of ~1–1.5 Å from the start structure (Fig. 4). The arrangement of the catalytic triad as well as residues 59 and 217 in the simulations of the wild type and double mutant are shown in Fig. 5. Although residue 59 is

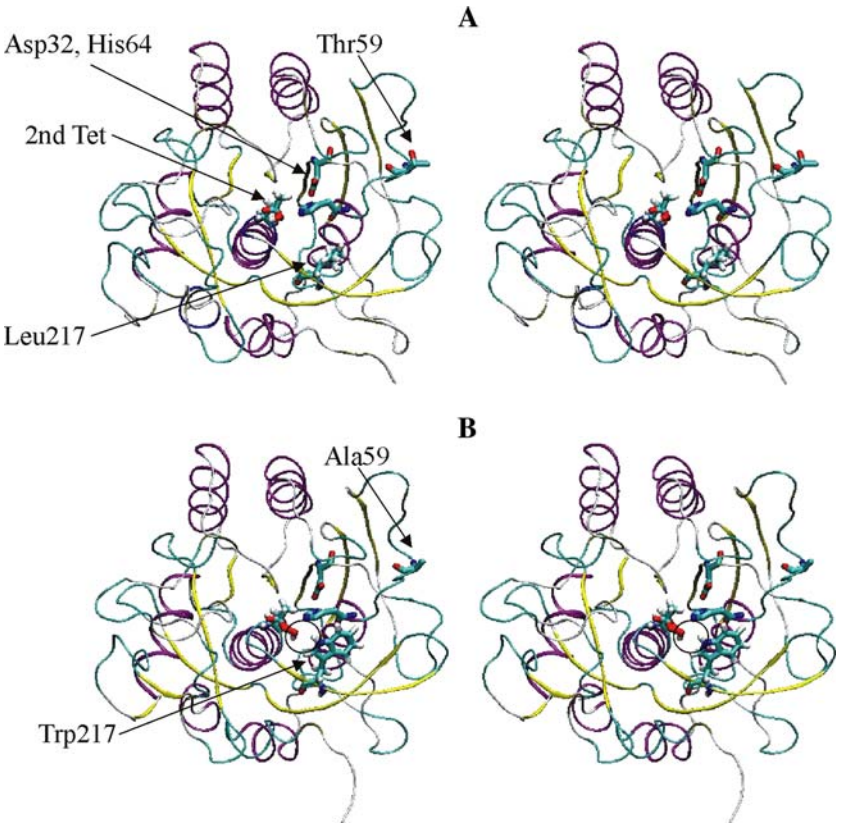

Fig. 5 Stereo view of the subtilisin Carlsberg wild type structure (**a**) and of the T59A/L217W mutation (**b**, cartoon representation of snapshots after ~1 ns MD simulation). The active site residues Asp32, His 64 and the Ser221 (second TI of perhydrolysis reaction) are shown as stick models and indicated by arrows. In addition, the location of the Leu217 and Thr59 (in **a**) and mutated residues Trp217 and Ala59 (in **b**) are indicated. The possible formation of a hydrogen bond between the peroxy-atom of the second TI and the Nε-H of Trp217 in the mutant is encircled (in **b**)

far from the active site and the side chain points towards the solvent a possible long-range influence of the T59A substitution cannot be excluded. However, the distance between either T59 (wild type) or A59 (mutant) and the second TI (Cα–Cα distance between residue 59 and Ser221 with the attached second TI) remained close to the starting distance during all simulations (18.7 ± 1.2 Å) and no structural rearrangements due to the T59A substitution were observed during the simulations. It is important to note that this does not exclude the possibility of a T59A influence that may occur on much longer time scales than the present MD simulations.

During the of MD simulation of the T59A/L217W mutant, it was observed that the second oxygen atom (O2) in the perhydroxyl group interacted with the Nε-hydrogen (Nε-H) atom of the Trp217 residue as shown in Figs. 5 and 6. The distance between these two atoms was monitored (Fig. 7). The length can act as a qualitative indicator of the strength of a hydrogen bond although its absolute strength also depends on other parameters like hydrogen bond angle. Additionally, in order to examine whether this hydrogen bond can be selectively formed during the perhydrolysis reaction or also in case of the second TI state of the hydrolysis reaction, we performed the equivalent simulations in case of a bound second TI for the hydrolysis reaction. The distance distribution between Trp217:Nε-H and oxygen atom in the perhydroxyl group was shifted to smaller distances compared to the corresponding distance between Trp217:Nε-H and the oxygen atom in the TI for the hydrolysis reaction (>4 Å for the majority of sampled conformations). This effect was seen for 4 ns data gathering times as well as during an extension to 8 ns data gathering (Fig. 7). The observed average distances are, however, larger than found for the interaction of the perhydroxyl hydrogen and the carbonyl oxygen in residue 28 of the aryl-esterase mutant (previous paragraph) but still allowing for selective stabilization of the second TI state of perhydrolysis reaction. Interestingly, for the distance distribution between Trp217:Nε-H and oxygen atom in the intermediate for the hydrolysis reaction a small peak around 2 Å was found (both during 4 and 8 ns data gathering) indicating that even in this case transient stable hydrogen bonding is possible. This result is consistent with the observation that even the mutant enzyme shows not exclusively perhydrolysis but also some hydrolysis activity [16]. The van der Waals presentation of Trp217 and the second TI illustrates this interaction but also demonstrates that an optimal hydrogen bond cannot be formed due to the sterical packing of the residues around the Trp217 (Fig. 6). The result demonstrates that for the T59A/L217W mutant the second TI state can be selectively stabilized only in case of the perhydrolysis but not or to a lesser degree in case of the hydrolysis reaction.

3.3 Interference with catalytically important hydrogen bonds

In addition to monitoring the hydrogen bonding between Trp217 and the O2 of the second perhydrolysis intermediate other hydrogen bonding distances were monitored during the simulations. A hydrogen bond between the Nε-H of His64 and the side chain OG atom of Ser221 is of critical importance for the progression of the hydrolysis as well as perhydrolysis reaction illustrated in Fig. 8a, b. During the reaction cycle the hydrogen at the Nε of His64 moves eventually to the OG of Ser221 to allow the product to leave the active site. Any competing hydrogen bond to His64:Nε-H may interfere and could potentially inhibit the reaction [7]. In case of the hydrolysis intermediate there is the oxygen (of the OH group, Fig. 8) that may interfere and in case of the perhydrolysis intermediate interference can be due to interaction with O1 or O2 of the intermediate (Fig. 8a, b). In addition to the simulations of the mutant, the corresponding hydrogen bonding distance distributions were also recorded for simulations of the wild type enzyme with the hydrolysis and perhydrolysis second intermediate states.

This comparison is important in terms of efficiency of perhydrolysis reaction because the hydrolysis reaction competes with perhydrolysis reaction in the acyl-enzyme step. If a water molecule attacks the acyl-enzyme complex as a nucleophile instead of hydrogen peroxide, then the hydrolysis reaction takes place instead of perhydrolysis reaction as shown in Fig. 1.

In the case of the hydrolysis reaction by wild type subtilisin, the curve representing the catalytically important hydrogen bonding interaction between His64 and Ser221 showed a peak around 2.0 Å and was well separated from the curve representing the interaction between His64 and the oxygen of the hydroxyl group (Fig. 8c). This indicates that the catalytically important interaction for the hydrolysis reaction is not interfered by other putative interactions in the case of wild type. However, surprisingly in the case of T59A/L217W mutant, the interaction between the oxygen atom of the hydroxyl group and His64 appeared to be stronger than the catalytically important interaction (compare distance distributions in Fig. 8e). Here, we again interpret a shift in the hydrogen bonding distance distribution as a qualitative measure of an interaction. This implies that the T59A/L217W mutant also inhibits the hydrolysis reaction due to strong interference by a competing hydrogen bond. Indeed, experimentally a reduced hydrolysis rate was obtained for the double mutant compared to wild type [16; and unpublished experimental results].

Interestingly, a further analysis of the hydrogen bonding distributions in case of the simulations with the second

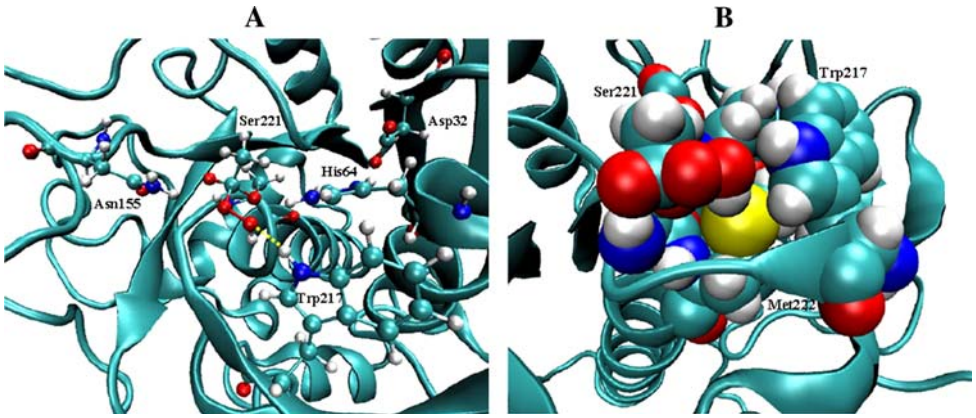

Fig. 6 **a** Snapshot from the MD simulation of the second TI state of the perhydrolysis reaction in case of the subtilisin T59A/L217W mutant. Residues important for catalysis and stabilization of the intermediate are shown in *ball* and *stick* representation (backbone as cartoon), and the interaction between the perhydroxyl group and Trp217 is indicated as *yellow dotted line*. **b** Same structure but from a different viewpoint (rotated by about 90°) and side chains represented by van der Waals spheres indicating the tight packing of residues around the Trp217 side chain

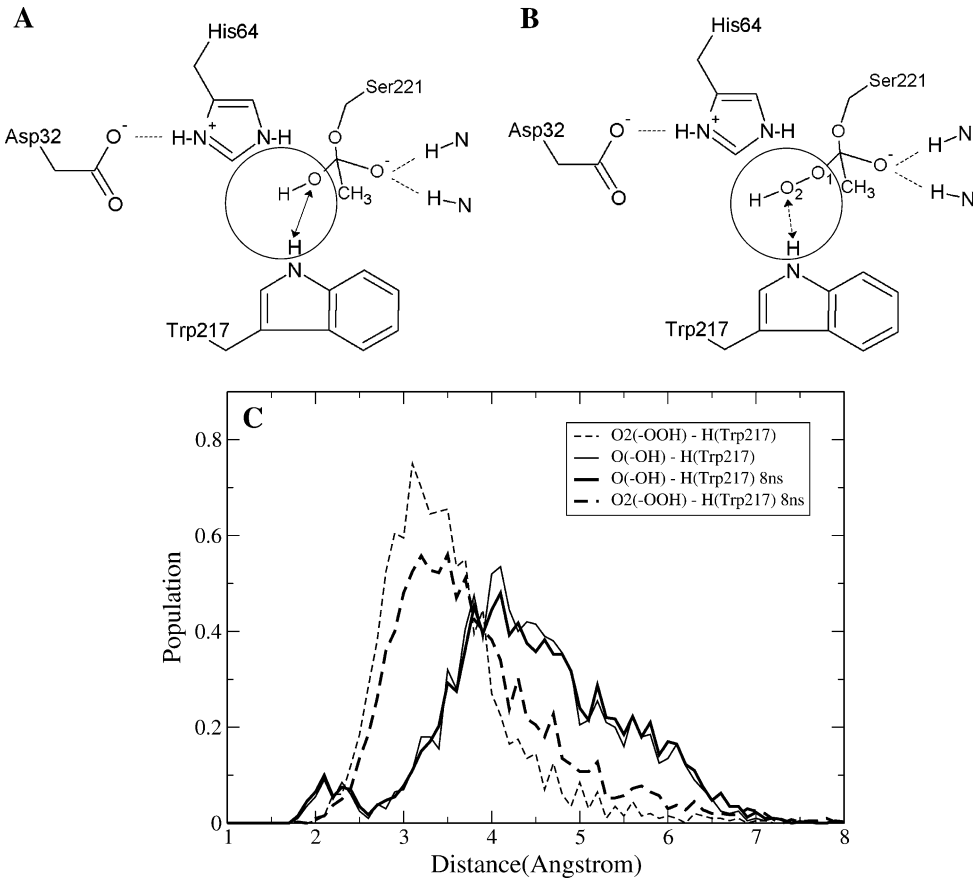

Fig. 7 Hydrogen bonding between Nε-H in Trp217 and the hydroxyl oxygen of the second TI of the hydrolysis and perhydrolysis reaction in the subtilisin Carlsberg T59A/L217W mutant. The chemical structure of the second TI states of the hydrolysis and perhydrolysis reactions are shown in (**a**) and (**b**), respectively. Relevant atoms that form putative hydrogen bonds are encircled. The interaction between the Nε-H in Trp217 and the oxygen of the hydroxyl group and of the O2 of the perhydroxyl group are indicated (*double arrows* in **a**, **b**) and the corresponding distance distributions are given in (**c**) as continuous and dashed lines, respectively (for 4 and 8 ns data gathering time periods)

intermediate of the perhydrolysis reaction gives also an explanation as to why the perhydrolysis reaction does not optimally occur in wild type subtilisin Carlsberg but is possible in case of the mutant. The distance distributions in the wild type case demonstrate a significant population of conformations compatible with hydrogen bond formation of the O1 and O2 of the second intermediate with the Nε-H of His64 (peaks at around 2.0 Å, Fig. 8d) indicating possible strong interference with the progression of the perhydrolysis reaction. Thus, the results shown here exactly agree with one of the reasons why subtilisin has only limited perhydrolase activity. Similar to wild type, the catalytically important interaction is also interfered in the case of T59A/L217W mutant (Fig. 8f) but to a lesser

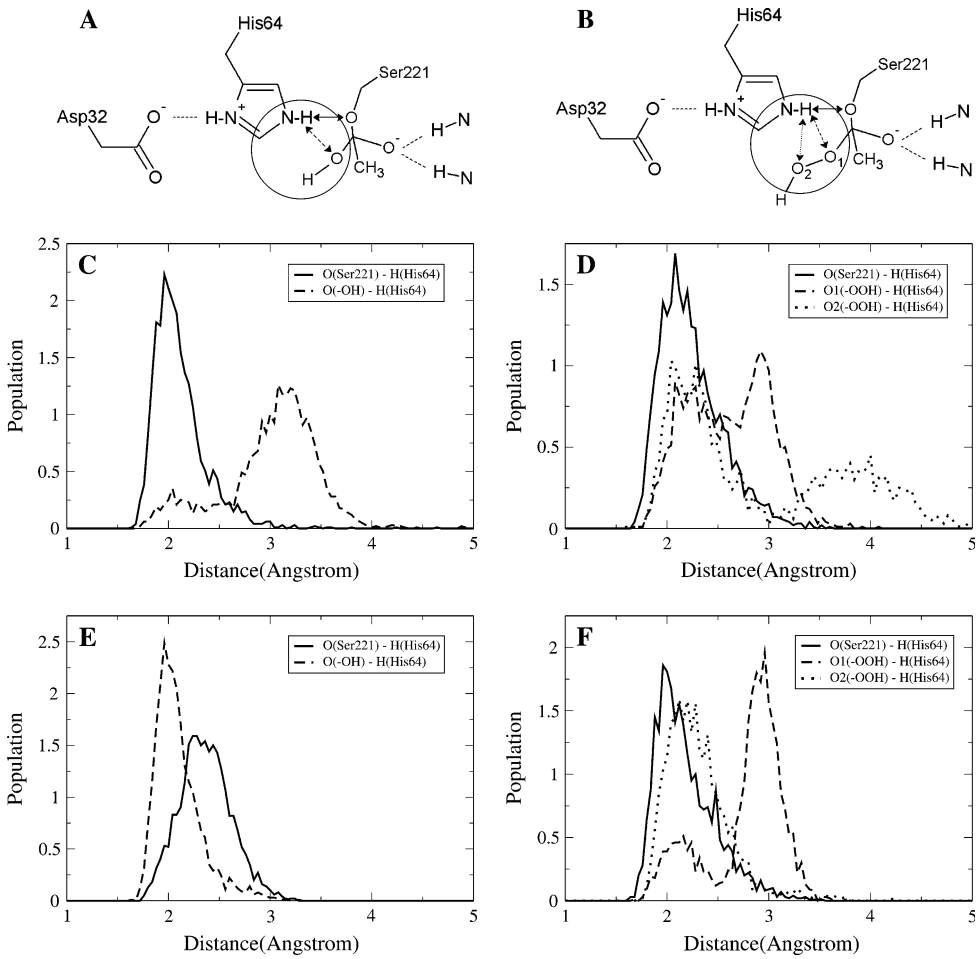

Fig. 8 Hydrogen bonding between His64 (hydrogen attached to Nε) and oxygen atoms in MD simulations of the second TI state of hydrolysis reaction (**a**) and perhydrolysis reaction (**b**). The putative hydrogen bonds are indicated in **a** and **b** (*double arrows*; relevant region encircled). The corresponding distance distributions recorded during the MD simulations are plotted in (**c** wildtype) and (**e** T59A/L217W mutant) for the second TI of the hydrolysis and for the perhydrolysis reaction (**d** wildtype) and (**f** T59A/L217W mutant), respectively

degree and involves mainly the oxygen atom (O2) in the perhydroxyl group which cannot accept the hydrogen. This result predicts an overall less efficient catalysis of the wild type compared to mutant.

4 Conclusions

In the present study, the stabilization of the second TI for hydrolysis and perhydrolysis reaction of wildtype subtilisin Carlsberg and a T59A/L217W double mutant was investigated using classical MD simulations. The aim was to relate the observed perhydrolysis activity of the mutant (no activity in wild type) to the hydrogen bonding pattern that stabilizes the second TI state. The results of all simulations are summarized in Table 1. Classical force field descriptions of TIs of serine hydrolases have been used already successfully to study lipases [35]. It should be emphasized that the characterization using a classical force field description of the hydrogen bonding pattern for the stabilization of intermediate states may not be accurate enough to draw quantitative conclusions on the stabilization [36]. However, we are primarily interested in a qualitative characterization of the hydrogen bonding pattern and how it could be affected by residue substitutions near the active site based on classical MD simulations that are much less demanding than QM or QM/MM methodologies [36]. The classical MD simulations can give hints on the influence of substitutions on the enzyme properties and could be helpful for designing enzyme mutants with further improved perhydrolysis activity. The MD simulations showed that the L217W mutation could be of key importance for stabilizing the second TI for the perhydrolysis reaction. The T59A mutation is located ~18.5 Å away from the active site (in terms of Cα–Cα distance of residue 59 and Ser221) and the side chain points towards the solvent. During the MD simulations no significant difference of the local structure at residue 59 between wild type and mutant was found. In addition, no significant differences in the distance of residue 59 and active site in the wild type versus mutant enzymes were observed during the simulations. Unfortunately, experimental data on a single T59A mutation is not available so that the possibility of any indirect long-range effect on the enzyme cannot be excluded. The simulations demonstrated that the Trp 217 can form a weak hydrogen bond with the O2 of the second

Table 1 Molecular dynamics simulations on aryl-esterase and subtilisin Carlsberg

Simulation system	H-bond pattern/possible influence on catalysis
Aryl-esterase (wt) + second TI (perhydrolysis); 1 ns + 4 ns	Trp28:CO–HO_2O_1-second TI- distance >3.5 Å
Aryl-esterase(L29P) + second TI (perhydrolysis); 1 ns + 4 ns	Trp28:CO–HO_2O_1-second TI- distance <2.5 Å
Subtilisin C. (wt) + second TI (perhydrolysis); 1 ns + 4 ns	No H-bond between second TI:O2 and Leu217; H-bond between His64:Nε-H and second TI:O1 and O2 (interference with catalytically important H-bond)
Subtilisin C. (wt) + second TI (hydrolysis); 1 ns + 4 ns	No hydrogen bond between second TI:HO and Leu217; stable catalytically important H-bond between His64:Nε-H and Ser221(second TI):OG; no interfering H-bond
Subtilisin C. (T59A,L217W) + second TI (perhydrolysis) 1 ns + 4/8 ns	Weak H-bond between second TI:O_2 and Trp217:Nε-H; only partial H-bond between second TI:O_1 and His64:Nε-H (weak interference with catalytically important H-bond)
Subtilisin C. (T59A,L217W) + second TI (hydrolysis) ; 1 ns + 4/8 ns	Very limited H-bond formation of second TI:OH and Trp217:Nε-H; significant H-bond between second TI:OH and His64:Nε-H (strong interference with catalytically important H-bond)

TI for the perhydrolysis reaction, but the analogous hydrogen bond is not formed in case of the second TI for the hydrolysis reaction. In case of the wild type no hydrogen bonding partner for stabilizing the perhydrolysis intermediate is available. Interestingly, simulations on the L29P mutation in the aryl-esterase from *P. fluorescens* (PFE) which has a 28 times higher perhydrolysis activity than the wild type enzyme also indicated a specific stabilization of the perhydrolysis intermediate (by a hydrogen bond between backbone carbonyl and the hydrogen of the perhydroxyl group) [7].

In addition, the MD simulations also revealed interesting differences of the hydrogen bonds formed between the hydrogen attached to Nε of the catalytically important His64 and the second TI. This hydrogen is of major importance to close the catalytic cycle (summarized in Table 1). In case of the hydrolysis reaction the hydrogen should interact with the oxygen of Ser221 for transfer to form the hydroxyl group of Ser221 after completion of the hydrolysis reaction. Any competing hydrogen bond may interfere with the catalysis. Indeed, in case of the wild type subtilisin the simulation indicated an almost perfect and specific interaction of the His64 Nε-H and the OG of Ser221 with no interfering hydrogen bonds. But in case of the T59A/L217W mutation the simulations indicated strong competition to form a hydrogen bond between His64:Nε-H and the oxygen of the hydroxyl group of the second TI. This result gives an excellent qualitative explanation for the reduced hydrolysis activity of the subtilisin mutant which cannot be explained by the observed stabilization of the second TI for the perhydrolysis reaction. In case of the second TI for the perhydrolysis reaction again partially opposing behavior of wild type and mutant were observed. The simulations revealed significant interference of the His64–Ser221 interaction necessary to complete the catalytic cycle with an interaction of the His64:Nε-H and the first oxygen (O1) of the perhydroxyl group in the second TI (for the wild type enzyme). This corresponds to a strongly interfering interaction since transfer of the hydrogen to this oxygen results in the backward reaction. Hence, in the wild type enzyme in addition to the absence of any specific stabilization of the second perhydrolysis intermediate the results indicate also a strong interfering interaction that prevents completion of the catalytic cycle.

However, in the case of the T59A/L217W mutation much less possible interference by the O1 was observed. Interference due to interactions with the O2 of the perhydroxyl group is of less importance because transfer of the hydrogen to this oxygen is not possible. Thus the simulations also give a qualitative indication as to why the T59A/L217W mutant can but the wild type enzyme cannot effectively complete the catalytic cycle in case of the perhydrolysis reaction.

Aim of the present study was not to simulate directly the catalytic enzyme reaction which requires a quantum mechanical treatment of the second TI and the residues involved in the reaction. However, even a classical comparative treatment of the second TI for the hydrolysis and perhydrolysis reaction and its stabilization by hydrogen bonding to functional groups of the enzyme gives several qualitative explanations of the functional differences of wild type and mutant subtilisin. The results can be very helpful for guiding the design of new enzyme variants to further improve the perhydrolysis capacity of the enzyme. For example, only a weak but specific stabilization of the second TI of the perhydrolysis reaction was observed for the T59A/L217W mutant by a hydrogen bond between Trp217–Nε-H and the O2 of the perydroxyl group due to the tight packing of the Trp217 side chain. It is likely that replacement of residues around Trp217 by residues with smaller side chains will further improve the ability of

Trp217 to stabilize the second intermediate by hydrogen bonding. Experimental studies of such enzyme variants are subject of ongoing work in our laboratory.

Acknowledgments This work was performed using the computational resources of the CLAMV (Computer Laboratories for Animation, Modeling and Visualization) at Jacobs University Bremen and supercomputer resources of the EMSL (Environmental Molecular Science Laboratories) at the PNNL (Pacific Northwest National Laboratories).

References

1. Polgar L (1971) Transformation of a serine protease of *Aspergillus oryzae* into a thiol-enzyme. Acta Biochim Biophys Acad Sci Hung 5:53–55
2. O'Brien PJ, Herschlag D (1999) Catalytic promiscuity and the evolution of new enzymatic activity. Chem Biol 6:R91–R105
3. Carboni-Oerlemans C, Dominguez de MP, Tuin B, Bargeman G, van der Meer A, van Germert R (2005) Hydrolase-catalysed synthesis of peroxycarboxylic acids: biocatalytic promiscuity for practical applications. J Biotech 126:140–151
4. Björkling F, Frykman H, Godtfredsen SE, Kirk O (1992) Lipase catalyzed synthesis of peroxycarboxylic acids and lipase mediated oxidations. Tetrahedron 48:4587–4592
5. Kirk O, Christensen MW, Damhus T, Godtfredsen SE (1994) Enzyme-catalyzed degradation and formation of percarboxylic acids. Biocatalysis 11:65–77
6. Zacks A, Klibanov AM (1985) Enzyme-catalyzed processes in organic solvents. Proc Natl Acad Sci USA 82:3192–3196
7. Bernhardt P, Hult K, Kazlauskas RJ (2005) Molecular basis of perhydrolase activity in serine hydrolases. Angew Chem Int Ed 44:2742–2746
8. Franssen MCR, van der Plas HC (1992) Haloperoxidases—their properties and their use in organic synthesis. Adv Appl Microbiol 37:41–99
9. Butler A, Walker JV (1993) Marine haloperoxidases. Chem Rev 93:1937–1944
10. Picard M, Gross J, Luebbert E, Toelzer S, Krauss S, van Pee KH, Berkessel A (1997) Metal-free bacterial haloperoxidases as unusual hydrolases: activation of H_2O_2 by the formation of peracetic acid. Angew Chem Int Ed 36:1196–1199
11. Hecht HJ, Sobek H, Haag T, Pfeiffer O, van Pee KH (1994) The metal-ion-free oxidoreductase from *streptomyces aureofaciens* has an α/β hydrolase fold. Nat Struct Biol 1:532–537
12. Pelletier I, Altenbuchner J, Mattes R (1995) A catalytic triad is required by the non-heme haloperoxidases to perform halogenation. Biochim Biophys Acta, Prot Struct Mol Enzymol 1250:149–157
13. Pelletier I, Altenbuchner J (1995) A bacterial esterase is homologous with non-heme haloperoxidases and displays brominating activity. Microbiology 141:459–468
14. Kirk O, Conrad LS (1999) Metal-free haloperoxidases: fact or artifact? Angew Chem Int Ed 38:977–979
15. Cheeseman JD, Tocilj A, Park S, Schrag JD, Kazlauskas RJ (2004) Structure of an aryl esterase from *Pseudomonas fluorescens*. Acta Cryst Sect 60:1237–1243
16. Wieland S, Polanyi-Bald L, Prueser I, Stehr R, Maurer KH (2005) Subtilisin variants with improved perhydrolase activity. USPTO 424070140
17. Fitzpatrick PA, Ringe D, Klibanov AM (1994) X-ray crystal structure of cross-linked subtilisin Carlsberg in water vs. acetonitrile. Biochem Biophys Res Commun 198:675–681
18. Stoll VS, Eger BT, Hynes RC, Martichonok V, Jones JB, Pai EF (1998) Differences in binding modes of enantiomers of 1-acetamido boronic acid based protease inhibitors: crystal structures of gamma-chymotrypsin and subtilisin Carlsberg complexes. Biochemistry 37:451–462
19. Guex N, Peitsch MC (1997) SWISS-MODEL and the Swiss-PdbViewer: an environment for comparative protein modelling. Electrophoresis 18:2714–2723
20. Case DA, Cheatham TE 3rd, Darden T, Gohlke H, Luo R, Merz KM Jr, Onufriev A, Simmerling C, Wang B, Woods RJ (2005) The Amber biomolecular simulation programs. J Comput Chem 26:1668–1688
21. Duan Y, Wu C, Chowdhury S, Lee MC, Xiong G, Zhang W, Yang R, Cieplak P, Luo R, Lee T (2003) A point-charge force field for molecular mechanics simulations of proteins. J Comput Chem 24:1999–2012
22. Frisch MJ, Trucks GW, Schlegel HB, Scuseria GE, Robb MA, Cheeseman JR, Montgomery Jr JA, Vreven T, Kudin KN, Burant JC, Millam JM, Iyengar SS, Tomasi J, Barone V, Mennucci B, Cossi M, Scalmani G, Rega N, Petersson GA, Nakatsuji H, Hada M, Ehara M, Toyota K, Fukuda R, Hasegawa J, Ishida M, Nakajima T, Honda Y, Kitao O, Nakai H, Klene M, Li X, Knox JE, Hratchian HP, Cross JB, Bakken V, Adamo C, Jaramillo J, Gomperts R, Stratmann RE, Yazyev O, Austin AJ, Cammi R, Pomelli C, Ochterski JW, Ayala PY, Morokuma K, Voth GA, Salvador P, Dannenberg JJ, Zakrzewski VG, Dapprich S, Daniels AD, Strain MC, Farkas O, Malick DK, Rabuck AD, Raghavachari K, Foresman JB, Ortiz JV, Cui Q, Baboul AG, Clifford S, Cioslowski J, Stefanov BB, Liu G, Liashenko A, Piskorz P, Komaromi I, Martin RL, Fox DJ, Keith T, Al-Laham MA, Peng CY, Nanayakkara A, Challacombe M, Gill PMW, Johnson B, Chen W, Wong MW, Gonzalez C, Pople JA (2004) Gaussian 03, Revision C.02. Gaussian, Inc., Wallingford CT
23. Bayly CI, Cieplak P, Cornell WD, Kollman PA (1993) A well-behaved electrostatic potential based method using charge restraints for determining atom-centered charges: the RESP model. J Phys Chem 97:10269–10280
24. Wang J, Wolf RM, Caldwell JW, Kollman PA, Case DA (2004) Development and testing of general Amber force field. J Comput Chem 25:1157–1174
25. Jorgensen WL, Chandrasekhar J, Madura JD, Impey RW, Klein ML (1983) Comparison of simple potential functions for simulating liquid water. J Chem Phys 79:926–935
26. Ryckaert JP, Ciccotti G, Berendsen HJC (1977) Numerical integration of the Cartesian equations of motion of a system with constraints: molecular dynamics of n-alkanes. J Comput Phys 23:327–341
27. Wang JH (1970) Directional character of proton transfer in enzyme catalysis. Proc Natl Acad Sci USA 66:874–881
28. Satterthwait AC, Jencks WP (1974) The mechanism of the aminolysis of acetate esters. J Am Chem Soc 96:7018–7031
29. Bachovchin WW, Roberts JD (1978) Nitrogen-15 nuclear magnetic resonance spectroscopy. The state of histidine in the catalytic triad of.alpha.-lytic protease. Implications for the charge-relay mechanism of peptide-bond cleavage by serine proteases. J Am Chem Soc 100:8041–8047
30. Emsley J (1980) Very strong hydrogen bonding. Chem Soc Rev 9:91–124
31. Bachovchin WW (1985) Confirmation of the assignment of the low-field proton resonance of serine proteases by using specifically nitrogen-15 labeled enzyme. Proc Natl Acad Sci USA 82:7948–7951
32. Fujinaga M, Delbaere LTJ, Brayer GD, James MNG (1985) Refined structure of alpha-lytic protease at 1.7 A resolution. Analysis of hydrogen bonding and solvent structure. J Mol Biol 183:479–502

33. Sumi H, Ulstrup J (1988) Dynamics of protein conformational fluctuation in enzyme catalysis with special attention to proton transfers in serine proteinases. Biochim Biophys Acta 955:26–42
34. Ash EL, Sudmeier JL, Day RM, Vincent M, Torchilin EV, Haddad KC, Bradshaw EM, Sanford DG, Bachovchin WW (2000) Unusual 1H NMR chemical shifts support (His) C(epsilon) 1…O==C H-bond: proposal for reaction-driven ring flip mechanism in serine protease catalysis. Proc Natl Acad Sci USA 97:10371–10376
35. Otte N, Pocola M, Thiel W (2008) Force-field parameters for the simulation of tetrahedral intermediates of serine hydrolases. J Comput Chem 30:154–162
36. Topf M, Varnai P, Richards WG (2002) Ab initio QM/MM dynamics simulation of the tetrahedral intermediate of serine proteases: Insights into the active site hydrogen-bonding network. J Am Chem Soc 124:14780–14788